Modulation of Lipid Polymorphism by the Feline Leukemia Virus Fusion Peptide: Implications for the Fusion Mechanism†

Sarah M. A. Davies,*,‡ Raquel F. Epand,§ Jeremy P. Bradshaw,‡ and Richard M. Epand§

Department of Preclinical Veterinary Sciences, Royal (Dick) School of Veterinary Sciences, University of Edinburgh, Summerhall, Edinburgh EH9 1QH, Scotland, U.K., and Department of Biochemistry, McMaster University Health Sciences Centre, Hamilton, Ontario L8N 3Z5, Canada

Received January 28, 1998

ABSTRACT: The structural effects of the fusion peptide of feline leukemia virus (FeLV) on lipid polymorphism were studied, using differential scanning calorimetry (DSC), ^{31}P nuclear magnetic resonance (NMR), and time-resolved X-ray diffraction. This peptide lowers the bilayer to inverted hexagonal phase transition temperature, T_H, of dipalmitoleoylphosphatidylethanolamine (DiPoPE) at peptide mole fractions of up to 1.5×10^{-3} at pH 5.0 and at pH 7.4. The temperature at which isotropic ^{31}P NMR signals for monomethyldioleoylphosphatidylethanolamine (MeDOPE) first occurred is lowered by the FeLV peptide. The amount of isotropic signal seen at 40 °C is directly correlated to the peptide:lipid molar ratio. In the peptide-containing samples, more lipid remains in the isotropic state over the whole recorded temperature range. Isotropic ^{31}P NMR signals were observed for DiPoPE in the presence of the FeLV peptide for the entire recorded temperature range of 35−50 °C, while pure DiPoPE showed no significant amount of isotropic signal. X-ray studies of DiPoPE show the formation of a new lipid phase with peptide, which is not seen in the pure lipid samples. Disordering of the L_α phase is evidenced by broadening of the diffraction peaks, and the hexagonal cell parameter is decreased with peptide present. Our results suggest that the FeLV peptide is increasing the negative curvature of the lipid system, which is thought to be crucial to the formation of highly bent, high-energy structural fusion intermediates, such as the "stalk" model. Fusion activity for this putative fusogenic peptide was also demonstrated, using a resonance energy transfer (RET) lipid mixing assay. To our knowledge, this work provides the first published experimental evidence of both fusogenic activity and effects on lipid polymorphism for the FeLV fusion peptide.

Membrane fusion plays a vital role in a large and diverse number of essential biological processes. Despite this fact, the precise molecular events which occur during fusion are still not known. Specific catalysts can promote fusion, and these differ between individual fusion processes. Fusion proteins from enveloped viruses, such as influenza virus hemagglutinin (*1*, *2*) and gp160 from human immunodeficiency virus (*3*) are among the most thoroughly studied fusion catalysts. It has been proposed that, although the initial triggers for the fusion pathway show great diversity, the actual lipid changes which occur in the fusing membranes may be very similar indeed for many fusion systems (*4*). Thus, studies of one particular fusion pathway may have wide-ranging implications for fusion in all eukaryotic cells as well as for infective mechanisms of all intracellular parasites.

In order for two initally distinct membranes to fuse, the lipid molecules comprising the two bilayers must rearrange temporarily into highly curved intermediates at the fusion site. It was first suggested that fusion intermediates were formed during lipid transitions from the planar lamellar to curved, nonbilayer phases (*5*). Studies by Ellens et al. (*6*) revealed increased liposome fusion rates in the same temperature range in which Gagne et al. (*7*) observed isotropic ^{31}P NMR[1] resonances of the same lipid. Isotropic resonances are due to lipid structures of high curvature in which lateral diffusion of phospholipids can motionally average the chemical shift anisotropy. They correlate with the presence of lipidic particles, seen by electron microscopy (*7*, *8*), and with amorphous and inverted cubic phases, measured by

† We thank the Wellcome Trust for support: S.M.A.D. holds a Wellcome Trust Veterinary Research Training Scholarship. S.M.A.D. traveled to Canada on a Birrel−Gray Scholarship. Support from the Medical Research Council of Canada (Grant MT-7654) and the British Council for Canada is also gratefully acknowledged.

* Author to whom correspondence should be addressed.

‡ University of Edinburgh.

§ McMaster University Health Services Centre.

[1] Abbreviations: FeLV, feline leukemia virus; DiPoPE, dipalmitoleoylphosphatidylethanolamine; MeDOPE, monomethyldioleoylphosphatidylethanolamine; RET, resonance energy transfer; SIV, simian immunodeficiency virus; L_α, liquid crystalline lamellar phase; H_{II}, inverted hexagonal phase; T_H, $L_\alpha-H_{II}$ phase transition temperature; DSC, differential scanning calorimetry; ^{31}P NMR, ^{31}phosphorus nuclear magnetic resonance; HPLC, high-performance liquid chromatography; I_s, lipid structures producing isotropic NMR signals; T_i, temperature at which isotropic signals are first detected; d_L, lamellar phase unit cell repeat distance (*d* spacing); d_H, inverted hexagonal phase unit cell repeat distance (*d* spacing); AA, amino acid; R_0, spontaneous radius of curvature of the lipid monolayer; DG, diacylglycerol; MLV, multilamellar vesicle; SUV, small unilamellar vesicle; TMC, transmonolayer contact intermediate; NBD-PE, L-α-*N*-(4-nitrobenzo-2-oxa-1,3-diazole)-PE from egg; Rh-PE, L-α-*N*-(lissamine-rhodamine B sulfonyl)PE from egg; ILA, interlamellar attachment; DMSO, dimethyl sulfoxide.

S0006-2960(98)00227-X CCC: $15.00
Published on Web 03/28/1998

X-ray diffraction (*9*). These highly curved isotropic lipid arrangements may be fusion intermediates. Diacylglycerols (DGs), which are fusion promoters, lowered the threshold temperature at which isotropic structures occurred (*10*). Isotropic structures were observed in the presence of DGs (*11*). The fusion peptide of simian immunodeficiency virus (SIV) promoted the formation of isotropic structures, while a nonfusogenic mutant of this peptide did not (*12*). Similar results were seen with the fusion peptide from influenza virus hemagglutinin (*13*); the wild-type peptide increased isotropic phase formation, but only at fusogenic pH, while the two mutant nonfusogenic peptides studied did not. These isotropic lipid mesophases occur on the pathway from the lamellar phase to the inverted hexagonal (H_{II}) or ordered cubic phases. Correlations have been found between the inhibition of membrane fusion by certain compounds and their ability to raise the lipid bilayer to inverted hexagonal phase transition temperature (T_H) as measured by high-sensitivity DSC (*14*). Similarly, fusion promoters have been shown to lower T_H (*15*, *12*, *13*). While kinetically stable lipid phases such as H_{II} and bicontinuous cubic phases may not be involved in biological fusion, the first steps in their transition pathways from the lamellar phase may be very important, in particular the bilayer destabilization thus produced.

A number of models have been proposed for the molecular arrangements of the lipid in fusion intermediates. These are based on a combination of experimental findings and theoretical calculations of the energetics involved. The most recent model (*16*) suggests the initial formation of a highly bent modified stalk structure, composed of the outer lipid monolayers of each bilayer, which then converts to a transmonolayer contact intermediate (TMC). This intermediate can then evolve into either a fusion pore/cubic phase fomation or into H_{II} phases (*17*). There is much theoretical (e.g., *18*, *19*) and experimental evidence (e.g., *17*, *20*−*22*) to support this model. Recently, Lee and Lentz (*23*) have identified distinct kinetic steps in the fusion pathway, which support the stalk−pore hypothesis. The highly bent stalk structure would be likely to give rise to isotropic NMR signals. Fusion catalysts are thought to affect the kinetics of the phase transitions, and not the thermodynamic stability of the individual lipid phases themselves. Thus, a favoring of the conversion of the lipid bilayer to nonlamellar phases should enhance the rate of formation of the fusion stalk, while an alternative mechanism would be a change of partitioning of the TMC intermediate toward the fusion pore/cubic phase pathway, as suggested for the influenza virus fusion peptide (*24*).

Modeling studies have suggested that fusion peptides insert obliquely into target lipid membranes and thus destabilize lipid molecular packing (*25*). Longitudinal precession of the obliquely oriented peptide would lead to greater disruption of the bilayer center than of its surface, thereby increasing the negative curvature pressure, and hence favoring the formation of inverted lipid phases (*26*, *13*). We have studied the effect of the fusion peptide from feline leukemia virus (FeLV) on lipid polymorphism. FeLV is a pathogenic exogenous retrovirus of cats (*27*) and the main cause of nontraumatic death in adult domestic cats worldwide. The proposed fusion peptide of FeLV is the hydrophobic amino terminus of p15E, the transmembrane-like region of the viral envelope glycoprotein spike gp85 (*25*). Its amino acid sequence shows similarity to that of the known fusion peptide of SIV (*28*), and also to those of other leukemia-producing Retroviridae (Swiss Protein Data Bank). Using a resonance energy transfer (RET) lipid mixing assay, we have also demonstrated fusion activity for this peptide. To our knowledge, this is the first published experimental work using this fusion peptide. The results are discussed in the light of current concepts of the fusion mechanism.

MATERIALS AND METHODS

Dipalmitoleoylphosphatidylethanolamine (DiPoPE) and monomethyldioleoylphosphatidylethanolamine (MeDOPE) were purchased from Avanti Polar Lipids (Alabaster, AL). Thin-layer chromatography showed a single spot for each. L-α-*N*-(4-nitrobenzo-2-oxa-1,3-diazole)PE from egg (NBD-PE) and L-α-*N*-(lissamine-rhodamine B sulfonyl)PE from egg (Rh-PE) were also purchased from Avanti. Dimethyl sulfoxide (DMSO) was obtained from BDH Chemicals (Toronto, ON).

The FeLV 28 amino acid and SIV 12 amino acid peptides were synthesized by Albachem Ltd. (26 Craigleith View, Edinburgh, EH4 3JZ, Scotland, U.K.) using solid-phase synthesis. Their purities were >95%, as determined by analytical HPLC, Maldi−Tof mass spectrometry, and amino acid analysis.

The FeLV peptide sequence, obtained from the Swiss Protein Data Bank, was EPISLTVALMLGGLTVGGIA-AGVGTGTK. The lysine was included on the carboxy terminus to increase solubility. It is the next naturally occurring residue on p15E. The SIV peptide sequence was GVFVLGFLGFLA, which has been shown previously to promote lipid mixing and thus membrane fusion (*29*).

Preparation of Lipid and Lipid/Peptide Films. Weighed amounts of the required lipid, or lipid plus peptide, were vortexed thoroughly in chloroform. The peptide-containing samples were then sonicated until the peptide dissolved. The chloroform was evaporated using nitrogen gas, and the samples were then placed under vacuum for 4 h, followed by lyophilization overnight to remove any trace residual solvent. The resulting films were then suspended in buffer and vortexed vigorously at room temperature for 10 min. The buffers used for the DSC, NMR, and X-ray diffraction studies were 20 mM PIPES, 1 mM EDTA, 150 mM NaCl, and 0.002% NaN_3 for pH 7.4 samples, or 10 mM citrate, 0.15 M NaCl for pH 5.0 samples, and for the RET assays, 10 mM glycine, 0.1 mM NaCl, 0.1 mM EDTA for the pH 9.5 buffer, and 10 mM Hepes, 0.15 M NaCl, 1 mM EDTA for the pH 7.0 buffer.

Differential Scanning Calorimetry. The samples were made to a final DiPoPE concentration of 10 mg/mL, including varying peptide concentrations as required, and they and the reference buffer were degassed under vacuum just prior to use. Thorough mixing was applied to ensure a uniform sample suspension for injection into the sample chamber. An MC-2 high-sensitivity scanning calorimeter (Microcal Co., Amherst, MA) was employed, at a scan rate of 45 K/h. The sample chamber held 1.4 mL. Continuous heating scans were run from 25 through to 60 °C. A single van't Hoff component was used to fit the recorded bilayer

to hexagonal phase transition, and the reported transition temperature is that for the fitted curve.

^{31}P NMR. A Bruker drx500 spectrometer, operating at a frequency of 202.45 MHz with broad band proton decoupling, was used to obtain the spectra. Three freeze−thaw cycles were carried out prior to measurement to ensure that all the lipid present was in the lamellar phase and also to ensure full hydration of the dry MeDOPE and DiPoPE. The suspensions were then vortexed vigorously to produce a lipid paste and loaded into 5 mm diameter thin-walled NMR tubes. The high lipid concentration of 50 mg/mL aids the formation of nonbilayer phases. The lipid/peptide molar ratios were 100:1 or 200:1 for the peptide-containing samples. Samples were heated in 5 or 10 °C steps. An equilibration time of around 15 min was used after raising the sample temperature, which was maintained to within ± 0.1 °C by a Bruker B-VT 1000 variable temperature unit. A relaxation delay of 3 s was used between scans. Prior to Fourier transformation, exponential line-broadening of 100 Hz was applied.

X-ray Diffraction. The X-ray diffraction experiments were performed at station 8.2 of the synchotron radiation source at the Daresbury Laboratory. The radiation wavelength was 1.54 Å. A Teflon-lined brass chamber with mica windows was used as sample holder, and an external circulating water bath was used to control the sample temperature, which was continuously monitored via a thermocouple. The temperature of the sample cell was linearly increased from 30 to 70 °C, at a heating rate of 90 °C/h. All samples were at pH 7.4. Each temperature scan consisted of 120 frames of diffraction data. The XOTOKO program was used to correct the raw data. Corrections for sample thickness and variation in detector response were applied, and background counts were subtracted. Detector response was determined by measuring a fixed source, ^{59}Fe, for several hours, at the start and the end of data collection. The detector was calibrated for small angle scattering using rat tail collagen, mounted in a cell and lightly stretched, as a standard. Under these conditions, collagen has a unit cell size of 676.08 Å (*30*). The corrected data were then plotted using this calibrated *x*-axis.

Liposome Preparation for Fusion Studies. Liposomes were made from lipid films prepared as above, using pure MeDOPE for the unlabeled LUVs, and with 2 mol % of both NBD-PE and Rh-PE present for the labeled LUVs. The dried lipid films were suspended initially in an iso-osmotic glycine buffer at pH 9.5, at a lipid concentration of 20 mg/mL. After vigorous vortexing, the lipid suspensions were subjected to five freeze−thaw cycles, by immersion in liquid nitrogen for 2 min, followed by plunging into a water bath, at a temperature of 40−60 °C, until the samples thawed. Next the samples were filtered 10 times through two stacked polycarbonate membranes, of pore size 0.1 μm, (Nucleopore Corp., Pleasanton, CA), using a high-pressure extruder (Lipex Biomembranes Inc., Vancouver, Canada) to yield LUVs.

Lipid Mixing Fusion Assay. Lipid mixing was measured using the method of monitoring the change in the intensity of fluorescence which results from fluorescence energy transfer between the two bilayer-inserted probes, NBD-PE and Rh-PE (*31*). A SLM Aminco Bowman Series 2 Luminescence Spectrometer with excitation and emission slits of 4 nm was used. The LUVs were added, at a ratio of 1:9 labeled:unlabeled, into a continuously stirred fluorimeter cuvette containing Hepes buffer of pH 7.0 at 37 °C. The LUVs comprised 1% of the total volume in the cuvette. The final lipid concentration was 300 μM. There was no detectable change in pH on addition of LUVs, since the volumes of LUVs added were very small. The excitation wavelength used was 470 nm, and the emission of NBD was recorded at 530 nm. A baseline fluorescence was measured for these suspensions. The FeLV and SIV peptides were dissolved separately in DMSO at a concentration of 1 mg/mL. These stock solutions of peptide were added to LUV preparations in the fluorimeter cuvettes to give a final peptide concentration of 10 μM. DMSO alone was also used as a control. One hundred percent lipid mixing was obtained by addition of 10% Triton X-100 to a final concentration of 0.1%.

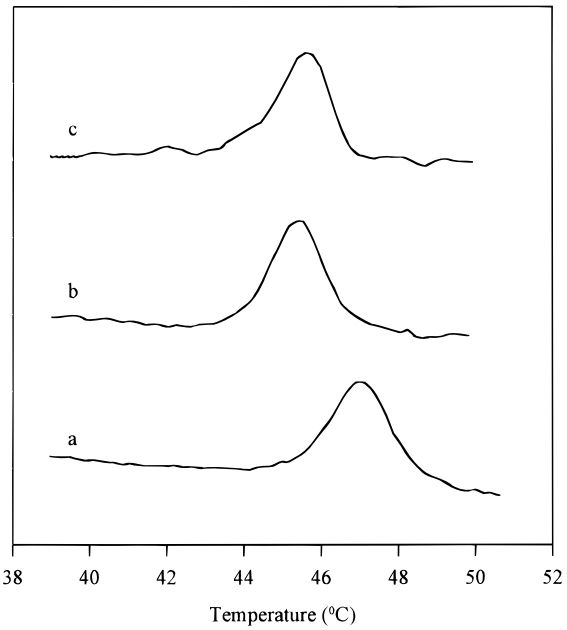

FIGURE 1: Some representative thermograms obtained at pH 7.4. Pure DiPoPE (a), DiPoPE with FeLV peptide present at a peptide mole fraction of 0.5×10^{-3} (b), and 0.65×10^{-3} (c). T_H is lowered in the presence of the FeLV fusion peptide. DSC heating scan rate was 45K/h.

RESULTS

Differential Scanning Calorimetry. Figure 1 shows three representative thermograms, at pH 7.4, from which values for T_H were obtained. It can be seen that T_H is lowered in the presence of both concentrations of FeLV fusion peptide shown. Plots of change in T_H with increasing peptide mole fraction, at pH 7.4 and pH 5.0, are shown in Figure 2, parts a and b, respectively. The resultant curves show an initial decrease in T_H, followed by an increase in T_H with consecutive rises in the peptide mole fraction. At peptide mole fractions of $>1.5 \times 10^{-3}$ a broadening of the enthalpy peaks was observed, indicating a decrease in cooperativity for this transition. The two pH curves are at least biphasic; obviously the possibility exists that these curves are described by more complex functions.

T_H is a measure of the relative stability of the L_α and H_{II} lipid phases. The reduction in T_H observed initially with increasing peptide concentration suggests that, at peptide mole fractions below 1.5×10^{-3}, this fusion peptide favors the formation of the H_{II} phase over the L_α phase at both pH

Table 1: Comparison of Effect of Viral Fusion Peptides on T_H of DiPoPE

viral fusion peptide	slope of line (°C/mole fraction peptide) at pH 5.0	slope of line (°C/mole fraction peptide) at pH 7.4
influenza HA2	-453 ± 112[a]	301 ± 49[a]
SIV	not studied	360 ± 100[b]
FeLV	-2128 ± 233	-1116 ± 444

[a] From Epand and Epand (*13*). [b] From Epand et al. (*12*).

5.0 and pH 7.4. The FeLV virus fuses with biological cells at pH 7.4 (*32*), so a decrease in T_H at both pH values is to be expected with this fusion peptide. Previous experiments which studied the effect of the influenza virus fusion peptide on T_H also found a difference with pH (13): the influenza virus fusion peptide lowered T_H at pH 5.0, but increased T_H at pH 7.4. These findings correlate with this peptide's pH-dependent fusogenic ability. In the same study of the influenza peptide, two nonfusogenic mutants were found to raise T_H, at both pH 5.0 and pH 7.4. DSC experiments performed using the SIV fusion peptide at pH 7.4 showed a decrease in T_H with the wild-type fusion peptide, and little change in T_H with a nonfusogenic mutant (*12*). This suggests that, at low peptide concentrations, a lowering of T_H is a fundamental property of viral fusion peptides. Table 1 shows the values of the slopes for the dependence of T_H on the mole fraction of fusion peptide for these three peptides: it should be noted that the range of peptide concentrations included here is not the same for FeLV as it is for the other two peptides studied, as we are only comparing the FeLV data which shows a reduction in T_H, i.e., the first half of the plotted results. This may explain in part why our gradients are so much steeper for the FeLV data. However, some of the quantitative differences between these values may be due to the difference in the structures of the fusion peptides. The FeLV peptide has an acidic residue on its amino terminus, the influenza peptide has several acidic residues along its length, and the SIV peptide has no polar residues. These factors will affect the depth and angle of peptide penetration into the lipid bilayer; alteration of the amino acid sequences of fusion peptides changes the membrane orientation of these peptides (*25*). Enhancement of H_{II} formation may be due to disruption of lipid packing and/or effects on lipid hydration, producing an increase in monolayer negative curvature strain (*33*). X-ray studies of the H_{II} phase lattice constant at constant temperature can determine whether alteration of the spontaneous radius of curvature of the lipid/water interface, R_0, occurs, and thus a change in monolayer negative curvature strain. This is seen for DiPoPE samples containing the FeLV peptide (see X-ray Diffraction Results).

T_H is seen to increase at FeLV peptide mole fractions above 1.5×10^{-3}, at both pH 5.0 and pH 7.4. We propose that this is due to increased self-aggregation of the extremely hydrophobic FeLV peptide molecules at these higher concentrations, thus preventing them, in part, from inserting into the lipid bilayers. Grossly, the peptide does appear to self-aggregate in these concentration ranges, as seen by the formation of gel-like masses in these samples by the end of the heating scans. A similar phenomenon has been observed with Amphotericin B, which is also extremely hydrophobic in nature (Epand, R. M., unpublished observation). T_H is

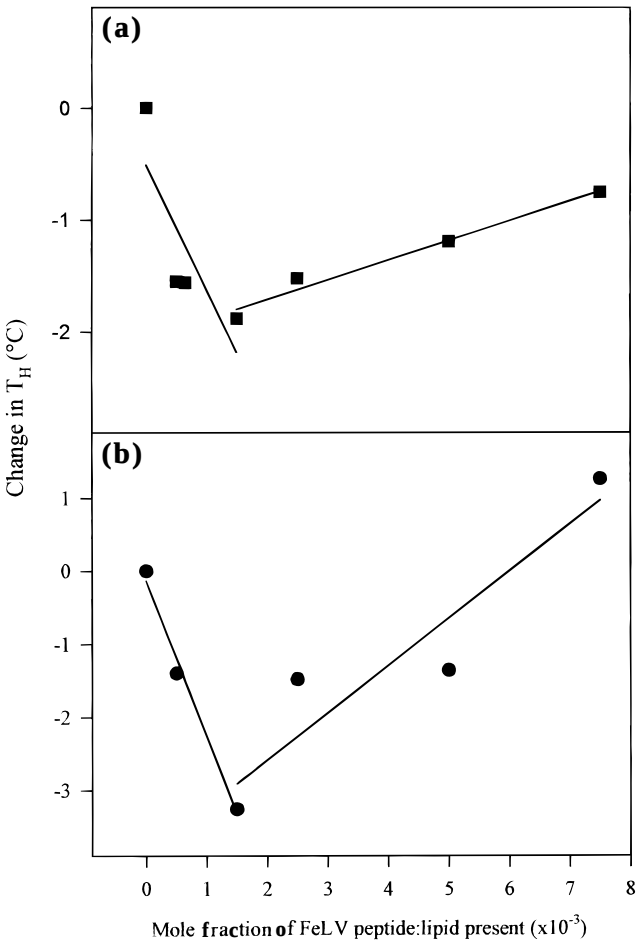

FIGURE 2: Change in lamellar to inverted hexagonal phase transition temperature of DiPoPE as a function of mole fraction of feline leukemia virus fusion peptide at (a) pH 7.4 (■) and (b) pH 5.0 (●).

seen to increase more in the presence of the FeLV peptide at pH 5.0 than at pH 7.4; presumably there is more self-aggregation of the peptide at this pH, possibly due to a decrease in negative charge of the glutamate residues at acidic pH. We suggest that the aggregated FeLV peptide fraction may lie along the bilayer surface, rather than insert into the membrane, and actually stabilize the L_α phase, possibly by reducing its negative curvature strain.

^{31}P NMR Spectroscopy. Figure 3 shows the ^{31}P NMR powder patterns obtained for pure MeDOPE and for MeDOPE plus FeLV fusion peptide as a function of temperature. The temperature at which isotropic resonances are first detected, T_i, drops with increasing peptide concentration. There is also a direct correlation between the mole fraction of peptide present and the amount of isotropic signal seen at 40 °C. Moreover, in the presence of the FeLV fusion peptide, a larger percentage of the lipid remains in this isotropic state over the full range of recorded temperatures. At 82 °C, a small amount of MeDOPE with FeLV peptide has converted to the H_{II} phase, whereas by 75 °C, the pure lipid already has a larger H_{II} signal. No significant differences were found between the pH 7.4 and the pH 5.0 samples. Figure 4 shows the ^{31}P NMR powder patterns obtained for pure DiPoPE and for DiPoPE plus FeLV fusion peptide as a function of temperature. The pure DiPoPE samples show no significant isotropic peak at any of the

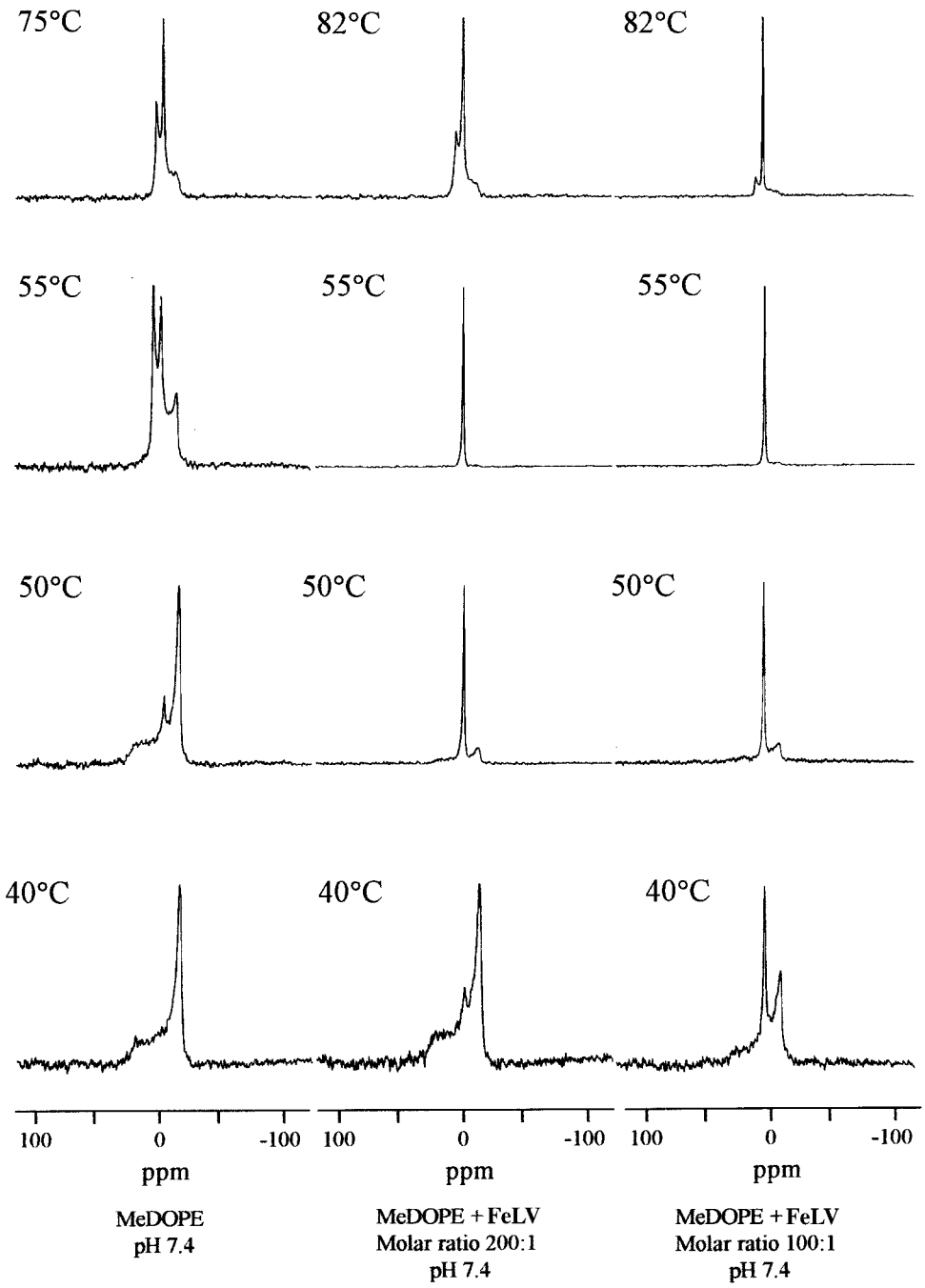

FIGURE 3: ^{31}P NMR spectra of pure MeDOPE, and samples containing different molar ratios of feline leukemia virus peptide, as a function of temperature. Lipid concentration in all samples is 50 mg/mL. Only pH 7.4 data are shown, but the pH 5.0 results were qualitatively similar.

recorded temperatures. However, in the presence of the FeLV peptide, a substantial isotropic component is seen throughout the entire recorded temperature range.

The shapes of ^{31}P powder patterns are determined by the extent of motional averaging, on the ^{31}P NMR time scale, of the chemical shift anisotropy of the ^{31}P atom present in the phospholipid headgroup. This, in turn, is directly influenced by the types of motion possible within the phospholipid dispersions. The amount of isotropic ^{31}P NMR resonance (I_s) present in the NMR spectrum has been directly correlated with the rate of membrane fusion between MeDOPE vesicles (*34*). Furthermore, the initial appearance of I_s has coincided with the start of membrane fusion (*35*). Similar findings have occurred with vesicles of different lipid compositions (*35*). Phospholipid molecules in inverted cubic phases generate isotropic ^{31}P NMR spectra (*36*). It is unlikely that ordered cubic phases are intermediates in fusion. Fusion intermediates are isolated structures, not phases. Furthermore, cubic phases have extreme kinetic stability (*37*). This view is supported by our NMR data, which show persistence of isotropic signals through a wide temperature range, over a period of hours. However, it has been suggested that fusion intermediates resemble intermediates formed on the pathway to cubic phase formation (*17*). Work with the fusion peptides from SIV (*12*) and influenza virus (*13*) showed enhancement of I_s in their presence. Our results presented here for the putative fusion peptide from FeLV suggest that it is indeed favoring the formation of lipid

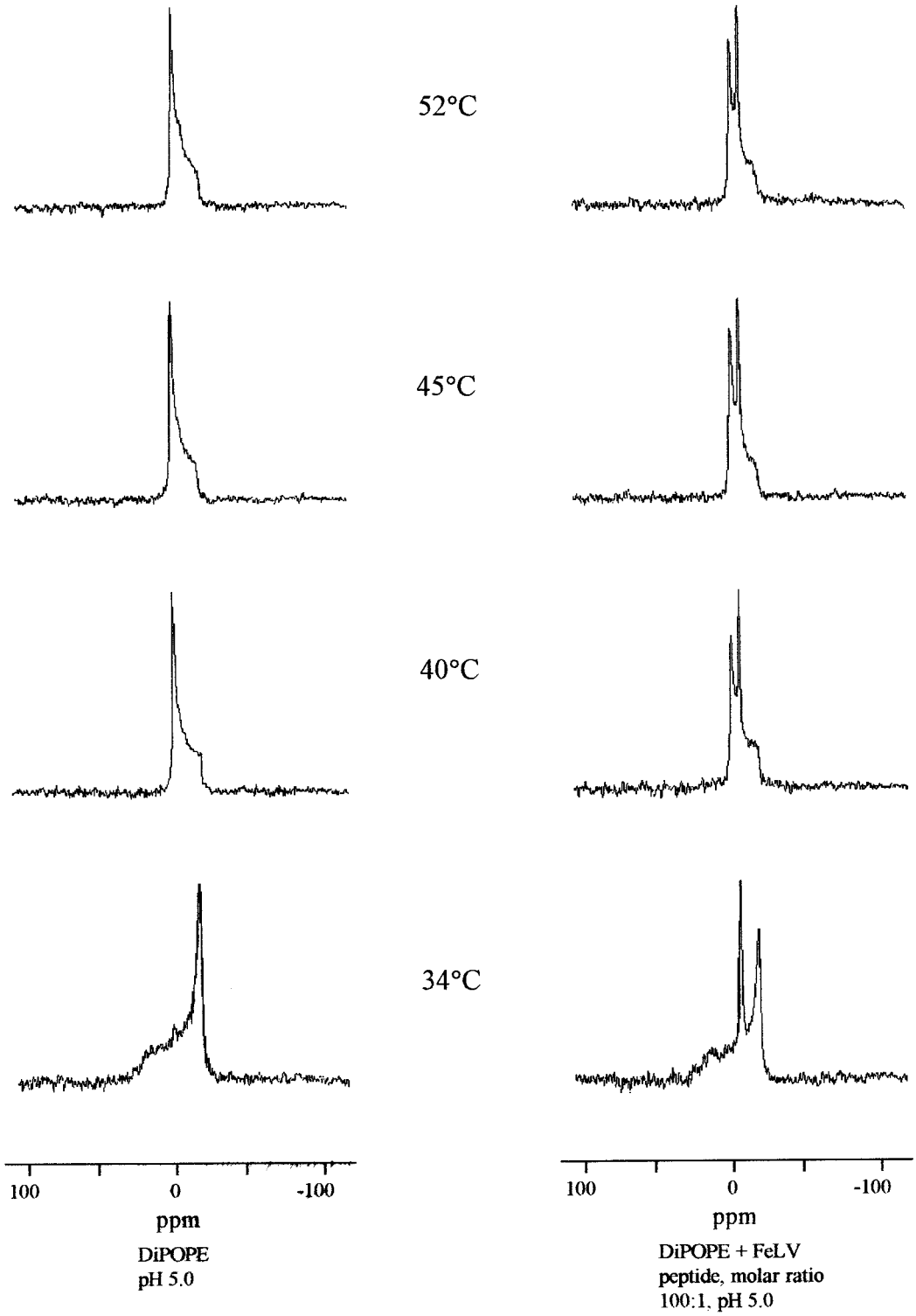

FIGURE 4: ^{31}P NMR spectra of DiPoPE alone and in the presence of a 100:1 molar ratio of lipid:FeLV peptide. Only pH 5.0 data are shown, but the pH 7.4 results were qualitatively similar. Lipid concentration in all samples is 50 mg/mL.

structures which are likely to be involved in the rate-limiting intermediate stages of the fusion pathway.

X-ray Diffraction Experiments. Time-resolved X-ray diffraction data were obtained to confirm the phase transitions measured by DSC and to determine any effects of the FeLV peptide on lipid structural parameters. The diffraction patterns verify that the transitions taking place in the DSC experiments are from L_α to H_{II}, no other phases being observed in the X-ray data. However, it is possible that very transient phases are not detected due to the high scan rate employed (disordered structures would not be seen either). Figure 5 shows a 3-dimensional plot of the series of diffraction patterns obtained for DiPoPE plus FeLV peptide present at a peptide mole fraction of 3.1×10^{-3} for the entire measured temperature range. Figure 6 shows a typical diffractogram for the T_H region of the scan; this was taken from the data for DiPoPE with FeLV peptide present at a peptide mole fraction of 1.6×10^{-3} and at 42 °C. Samples were assigned the H_{II} phase if a minimum of three diffraction peaks were observed which indicated spacings in the ratios

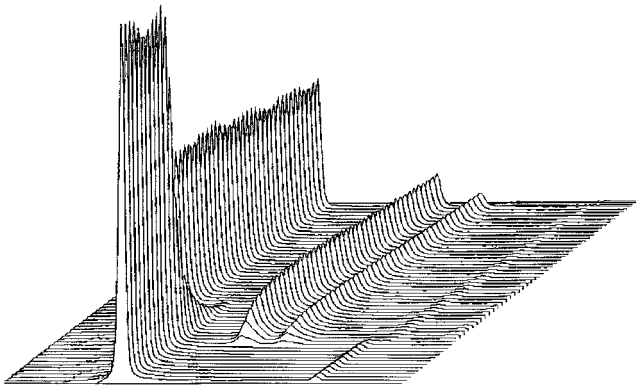

FIGURE 5: Three-dimensional plot of the series of consecutive diffraction patterns obtained on heating from 30 °C to 70 °C for DiPoPE plus FeLV fusion peptide, at a peptide mole fraction of 3 $\times$ 10^{-3}. The heating scan rate was 90 °C/h. The origin is on the left, and the right-hand limit represents channel 270 of the 512 recorded. The first two lamellar and first three hexagonal diffraction orders are visible as well-defined peaks. The transition from the lamellar to the hexagonal phase can be seen. The presence of a third, peptide-induced phase can be seen as a shoulder on the first and second hexagonal phase peaks.

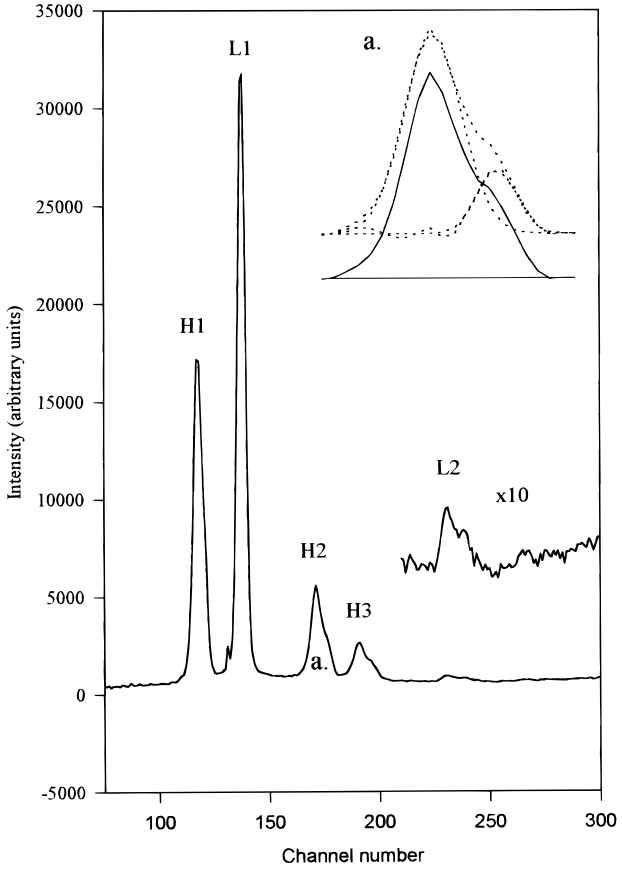

FIGURE 6: Typical small-angle X-ray diffraction profile in the T_H region of the scan series for DiPoPE plus FeLV fusion peptide at a peptide mole fraction of 1.6 $\times$ 10^{-3}, at 42 °C. Channel numbers 1−300 of the 512 recorded are shown. Part of the data has been amplified by a factor of 10 ($\times$10) for the sake of clarity. The inset, (a), shows an enlargement of the Bragg peak for the second diffraction order of the H_{II} phase, and the presence of a smaller peak, of smaller *d* spacing than the main H_{II} peak (solid lines). Gaussian analysis of the two peaks is shown above (dotted lines).

1:$\sqrt{3}$:$\sqrt{4}$:$\sqrt{7}$. The *d* spacings for all samples were calculated from the distance of peaks from the origin. The *d* spacings for the L_α and H_{II} phases for pure DiPoPE and the peptide-containing samples are plotted in Figure 7. The *d* spacings found in the present work are in good agreement with those previously reported (*24*, *38*). It should be noted that in the values presented in the references the definition used for the repeat spacing was that adopted by Gruner and others (*39*) in which the *d* space corresponds to the distance from the center of one H_{II} cylinder to the next. This distance is related to the lattice spacing reported in the present work by multiplying the lattice spacing by $2/\sqrt{3}$. The small differences between the two sets of data may be the result of different heating protocols, different batches of DiPoPE, and different calibrations. The transition from the L_α to the H_{II} phase is ordered, i.e., both lamellar and hexagonal phase domains coexist in the transition temperature region. This was seen for the pure lipid and the peptide-containing samples. No cubic intermediates are seen. The slow rate of water penetration into the nascent H_{II} phase seen with multilamellar vesicle (MLV) samples may prolong the detection of coexistence of L_α and H_{II} domains. Figure 6a (inset) shows the Gaussian analysis of the Bragg peak of the second diffraction order of the hexagonal phase. It can be seen that, in the presence of the FeLV peptide, a second and different lattice was observed, of slightly narrower *d* spacing than that of the main H_{II} phase. As one cannot assign a lipid phase on less than three diffraction orders, it is not possible to state definitely what this novel, peptide-induced phase is; there are only two observable diffraction peaks for this phase, which represent the second and third diffraction orders. The diffraction amplitudes of higher orders are too small to detect, and the first orders of the two hexagonal phases probably overlap due to the decrease in spatial resolution seen at smaller diffraction angles. This may account for the observed slight increase in mosaic spread of the first order of diffraction of the hexagonal phase in the presence of peptide. However, the two observed novel peaks fit to a *d* spacing of 1: $\sqrt{3}$, and they occur as a shoulder on the definitely identified main H_{II} phase. Thus, this may

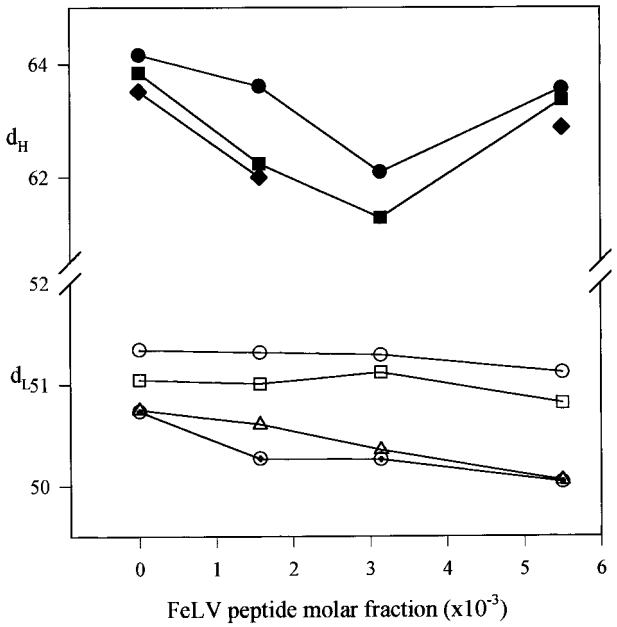

FIGURE 7: Variation in *d* spacings (Å) for the L_α and H_{II} phases of DiPoPE with increasing FeLV peptide concentration. d_H measured (●) at 49 °C, (■) at 50 °C, and (◆) at 52 °C. d_L measured (○) at 33 °C, (□) at 40 °C, (Δ) at 44 °C, and (⊕) at 45 °C.

represent a novel H_{II} phase, which was most noticeable in the 1.6×10^{-3} FeLV peptide mole fraction samples. A measure of the maximum percentage of DiPoPE present in this phase as a proportion of total amount of hexagonal phase lipid yielded the following data: 0% with no peptide present, 32%, 20%, and 21% at peptide mole fractions of 1.6×10^{-3}, 3.1×10^{-3}, and 5.5×10^{-3}, respectively. Evidence of the peptide-induced lattice disappeared completely as heating continued well above T_H, indicating that this phase is transient. No extra peaks were seen in the pure lipid samples, and thus it is clear that this novel phase is due to the presence of peptide. Not all of the peptide is incorporated into these domains, since the *d* spacing of the main H_{II} phase (d_H) is also decreased in the presence of the FeLV peptide (see Figure 7); this also suggests that the FeLV peptide is decreasing R_0 of the system in this peptide concentration range. A reduction in R_0 will destabilize bilayer structures relative to inverted nonbilayer phases. DGs have been found to decrease R_0, i.e., to increase the spontaneous negative curvature, of MeDOPE (*35*). Physiological levels of DGs are known to promote fusion (*40*) and have also been found to enhance a L_α to cubic phase transition (*11*), to bicontinuous Q^{224} (*41*). This cubic phase is related to the putative fusion intermediate, in the patch-the-puncture fusion model (*42*). An interesting observation in our experiments is that of marked broadening of the L_α diffraction peaks on heating in the presence of the FeLV peptide, and in a peptide concentration-dependent manner. (The width of the peaks was determined by fitting Gaussians and measuring the width at half-height). This represents disordering of the L_α phase and may be consistent with the start of a transition to an inverted cubic phase (*9*). X-ray studies of DiPoPE with an SIV mutant fusion peptide at pH 7.4 (*38*) and from influenza virus at pH 5.0 (*24*) have indeed detected the formation of a cubic phase. The heating scan rates used in these studies were considerably slower than that used here, which may explain why no ordered cubic phase was detected in our study. When rapid heating was used with the influenza fusion peptide, no cubic phase was observed (*24*). It has also been observed that, even with pure MeDOPE, the extent of cubic phase formation is very dependent on scan rate (*10*, *43*). The FeLV peptide also produced broadening of the H_Π peaks. Part of the peak broadening may be due to vesiculation of the multilamellar vesicles (MLVs) present in the samples, as suggested for the SIV fusion peptide/MeDOPE system; the conversion of MLVs to smaller vesicles with fewer lamellae is thermodynamically favorable, but the fusion peptide may greatly accelerate this process (*38*). The effect of the FeLV peptide on d_H is seen to exhibit a biphasic trend with peptide concentration, reminiscent of that seen for T_H in our DSC measurements. The fusion peptide had little effect on d_L at temperatures well below T_H, (see Figure 8), but as T_H is approached, d_L decreases with increasing peptide concentration. It can be seen from Figure 8 that the temperature-dependence of d_H and d_L is very similar for both pure lipid and the peptide-containing samples.

Fusion Assay. Figure 9 shows the percentages of lipid mixing between MeDOPE LUVs obtained in the presence of the SIV and FeLV fusion peptides. MeDOPE was used, since DiPoPE does not form stable liposomes. The SIV peptide promotes rapid lipid mixing (and thus membrane fusion) between the labeled and unlabeled LUV populations,

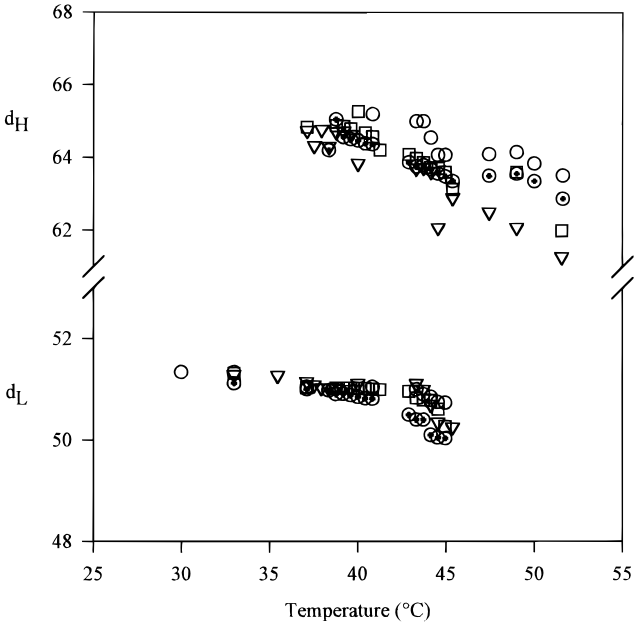

FIGURE 8: Change in *d* spacings (Å) of the L_α and H_Π phases with temperature as calculated from the X-ray diffraction patterns. DiPoPE alone (○); DiPoPE plus FeLV peptide at a peptide mole fraction of 1.6×10^{-3} (□), 3.1×10^{-3} (▽), and 5.5×10^{-3} (⊕).

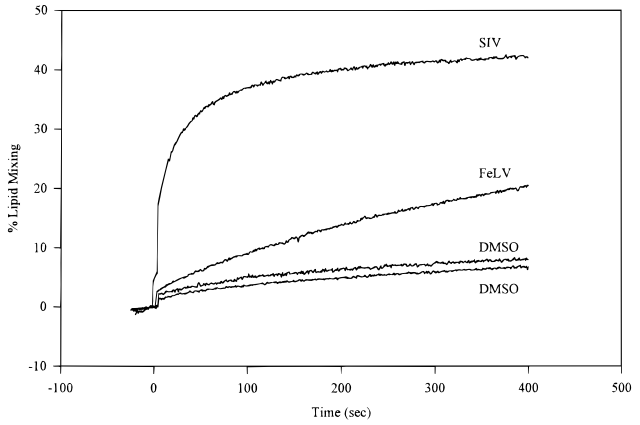

FIGURE 9: The percentages of lipid mixing between MeDOPE LUVs induced by the SIV and FeLV fusion peptides. The peptides, which were dissolved in DMSO, were added at time 0. Changes in fluorescence due to equivalent aliquots of the pure DMSO solvent are also shown. The top DMSO curve corresponds to 52 μL of added solvent as used for the FeLV peptide, and the bottom curve to 24 μL as used for the SIV peptide. Measurements were performed at 37 °C, and at pH 7.0.

as seen by the change in NBD fluorescence on probe dilution. Our results agree very closely with previous experiments performed using this peptide (*29*). The FeLV peptide also clearly produces membrane fusion, as shown by lipid mixing. The SIV peptide shows greater enhancement of fusion using this particular lipid system. This difference in potency may reflect the many differences between these two peptides, for example their lengths, overall electrical charges, solubility characteristics, and probable miscibilities with different lipid species. Moreover, different viral fusion peptides have been shown to require different specific experimental conditions in order to promote maximum membrane fusion (e.g., ref *44*−*46*). Thus, the experimental conditions used here may not provide optimal fusogenic conditions for the FeLV fusion peptide. The SIV fusion peptide was chosen as a control

since it is the most homologous retroviral fusion peptide for which there is definite experimental proof of fusogenic activity.

DISCUSSION

Two aspects of membrane fusion mechanisms can explain the relationship between a peptide-induced increase in membrane fusion rates and the effect of the peptide on lipid polymorphism. The first aspect is the formation of a stalk or interlamellar attachment (ILA) intermediate which has overall negative curvature (*16*). Thus the formation of this first intermediate would be accelerated by agents or conditions which favor the formation of inverted phases. The monolayers involved in the formation of this stalk intermediate are the trans or contacting monolayers (*22*). There are several examples of viral fusion peptides which lower T_H and therefore favor the formation of inverted phases, including both the SIV fusion peptide (*12*, *38*) and the influenza fusion peptide (*13*). In the present work we demonstrate, by DSC and X-ray diffraction, that the putative fusion peptide of FeLV can lower T_H of DiPoPE, at least at low peptide mole fractions. This peptide also causes d_H to decrease (Figure 7), indicating that the peptide promotes negative monolayer curvature.

Another mechanism by which peptides can promote the rate of fusion is by favoring the partitioning of the TMC intermediate toward the fusion pore/cubic phase pathway (*17*). This mechanism has been suggested for the influenza fusion peptide (*24*). The possibility of such a phenomenon occurring with the FeLV peptide is suggested by the fact that low concentrations of peptide promote the formation of isotropic resonances in ^{31}P NMR of MeDOPE and DiPoPE (Figures 3 and 4). Although no cubic phases were observed for DiPoPE by X-ray diffraction, this lipid forms cubic phases less readily. As a pure lipid, the cubic phase has never been observed with DiPoPE and in the presence of the influenza peptide the cubic phase is only found with DiPoPE mixed with other phases and with a low degree of order, presenting limited evidence for the formation of a cubic phase. The relationship between conditions leading to cubic phase formation and to increased rates of membrane fusion has also been noted with DAG-induced fusion (*11*, *47*).

The present work provides evidence that the N-terminus of the fusion protein of FeLV has effects on lipid properties which are characteristic of viral fusion peptides. It also demonstrates membrane fusion activity for the FeLV peptide, in the form of lipid mixing between liposomes. Furthermore, this peptide is an N-terminal segment, released by proteolytic activation of the fusion protein, which is also a feature shared with several other viral fusion peptides. The molecular mechanism by which it promotes fusion may depend on the nature of the target membrane and also on what the rate-determining step is in fusion. This peptide is suggested to accelerate both the rate of stalk formation as well as the partitioning of the TMC intermediate toward the formation of a fusion pore.

ACKNOWLEDGMENT

Grateful thanks to Mr. D. W. Hughes for technical assistance with NMR data collection, and to Dr. B. U. Komanschek for expert help with the running of station 8.2 at Daresbury.

REFERENCES

1. Bullough, P. A., Hughson, F. M., Skehel, J. J., and Wiley, D. C. (1994) *Nature 371*, 37.
2. White, J. M. (1995) *Cold Spring Harbor Symp. Quant. Biol. 60*, 581.
3. Freed, E. O., and Martin, M. A. (1995) *J. Biol. Chem. 270*, 23883.
4. Chernomordik, L. V., and Zimmerberg, J. (1995) *Curr. Opin. Struct. Biol. 5*, 541.
5. Papahadjopoulos, D., Vail, W. J., Newton, C., Nir, S., Jacobson, K., Poste, G., and Lazo, R. (1977) *Biochim. Biophys. Acta 465*, 579.
6. Ellens, H., Bentz, J., and Szoka, F. C. (1986) *Biochemistry 25*, 4141.
7. Gagné, J., Stamatatos, L., Diacovo, T., Hui, S. W., Yeagle, P. L., and Silvius, J. R. (1985) *Biochemistry 24*, 4400.
8. Hui, S. W., Stewart, T. P., and Boni, L. T. (1983) *Chem. Phys. Lipids 33*, 113.
9. Gruner, S. M., Tate, M. W., Kirk, G. L., So, P. T. C., Turner, D. C., Keane, D. T., Tilcock, C. P. S., and Cullis, P. R. (1988) *Biochemistry 27*, 2853.
10. van Gorkom, L. C. M., Nie, S.-Q., and Epand, R. M. (1992) *Biochemistry 31*, 671.
11. Basáñez, G., Nieva, J. L., Rivas, E., Alonso, A., and Goñi, F. M. (1996) *Biophys. J. 70*, 2299.
12. Epand, R. F., Martin, I., Ruysschaert, J. M., and Epand, R. M. (1994) *Biochem. Biophys. Res. Commun. 205*, 1938.
13. Epand, R. M., and Epand, R. F. (1994) *Biochem. Biophys. Res. Commun. 202*, 1420.
14. Epand, R. M. (1986) *Biosci. Rep. 6*, 647.
15. Siegel, D. P., Banschbach, J., and Yeagle, P. L. (1989) *Biochemistry 28*, 5010.
16. Siegel, D. P. (1993) *Biophys. J. 65*, 2124.
17. Siegel, D. P., and Epand, R. M. (1997) *Biophys. J. 73*, 3089.
18. Markin, V. S., Kozlov, M., M., and Borovjagin, V. L. (1984) *Gen. Physiol. Biophys. 3*, 361.
19. Kozlov, M. M., Leikin, S. L., Chernomordik, L. V., Markin, V. S., and Chizmadzhev, Y. A. (1989) *Eur. Biophys. J. 17*, 121.
20. Hui, S. W., Stewart, T. P., Boni, L., and Yeagle, P. L. (1981) *Science 212*, 921.
21. Melikyan, G. B., White, J. M., and Cohen, F. S. (1995) *J. Cell Biol. 131*, 679.
22. Chernomordik, L. (1996) *Chem. Phys. Lipids 81*, 203.
23. Lee, J. K., and Lentz, B. R. (1997) *Biochemistry 21*, 6251.
24. Colotto, A., and Epand, R. M. (1997) *Biochemistry 36*, 7644.
25. Brasseur, R., Vandenbranden, M., Cornet, B., Burny, A., and Ruysschaert, J.-M. (1990) *Biochim. Biophys. Acta 1029*, 267.
26. Epand, R. M., Cheetham, J. J., Epand, R. F., Yeagle, P. L., Richardson, C. D., Rockwell, A., and DeGrado, W. F. (1992) *Biopolymers 32*, 309.
27. Rojko, J. L., and Hardy, W. D. J. (1994) in *The Cat-Diseases and Clinical Management* (Sherding, R. G., Ed.) p 263, Churchill Livingstone Press, New York.
28. Bosch, M., Earl, P., Fargnoli, K., Picciafuoco, S., Giombini, F., Wong Staal, F., and Risser, R. (1989) *Science 244*, 694.
29. Martin, I., Dubois, M.-C., Defrise-Quertain, F., Saermark, T., Burny, A., Brasseur, R., and Ruysschaert, J.-M. (1994) *J. Virol. 68*, 1139.
30. Fraser, R. D. B., and MacRae, T. P. (1981) *Int. J. Biol. Macromol. 3*, 193.
31. Struck, D. K., Hoekstra, D., and Pagano, R. (1981) *Biochemistry 20*, 4093.
32. Laird, H. M., Jarrett, O., and Whalley, J. M. (1973) *Bibl. Haematol. 39*, 133.
33. Gruner, S. M. (1985) *Proc. Natl. Acad. Sci. U.S.A. 82*, 3665.
34. Yeagle, P. L., Young, J., Hui, S. W., and Epand, R. M. (1992) *Biochemistry 31*, 3177.

35. Ellens, H., Siegel, D. P., Alford, D., Yeagle, P. L., Boni, L., Lis, L. J., Quinn, P. J., and Bentz, J. (1989) *Biochemistry 28*, 3692.
36. Siegel, D. P., Banschbach, J., Ellens, H., Alford, D., and Bentz, J. (1989) *Biophys. J. 55*, 28A (Abstract).
37. Yeagle, P. L. (1994) *Curr. Top. Membr. 40*, 197.
38. Colotto, A., Martin, I., Ruysschaert, J.-M., Sen, A., Hui, S. W., and Epand, R. M. (1996) *Biochemistry 35*, 980.
39. Gruner, S. M. (1991) in *The Structure of Biological Membranes* (Yeagle, P., Ed.) p 211, CRC Press, Boca Raton, FL.
40. Siegel, D. P., Banschbach, J., Alford, D., Ellens, H., Lis, L. J., Quinn, P. J., Yeagle, P. L., and Bentz, J. (1989) *Biochemistry 28*, 3703.
41. Luzzati, V., Vargas, R., Mariani, P., Gulik, A., and Delacroix, H. (1993) *J. Mol. Biol. 229*, 540.
42. Nieva, J. L., Alonso, A., Basáñez, G., Goñi, F. M., Gulik, A., Vargas, R., and Luzzati, V. (1995) *FEBS Lett. 368*, 143.
43. Siegel, D. P., and Banschbach, J. (1990) *Biochemistry 29*, 5975.
44. White, J. M. (1990) *Annu. Rev. Physiol. 52*, 675.
45. Larsen, C. E., Nir, S., Alford, D. R., Jennings, M., Lee, K.-D., and Düzgünes, N. (1993) *Biochim. Biophys. Acta 1147*, 223.
46. Nieva, J. L., Nir, S., Muga, A., Goni, F. M., and Wilschut, J. (1994) *Biochemistry 33*, 3201.
47. Basáñez, G., Ruiz-Argüello, B., Alonso, A., Goñi, F. M., Karlsson, G., and Edwards, K. (1997) *Biophys. J. 72*, 2630.

BI980227V